Origin and suppression of back conversion in a phase-matched nonlinear frequency down-conversion process

Jingui Ma (马金贵), Jing Wang (王 静), Peng Yuan (袁 鹏)*, Guoqiang Xie (谢国强), and Liejia Qian (钱列加)

Key Laboratory for Laser Plasmas (Ministry of Education), Department of Physics and Astronomy, IFSA Collaborative Innovation Centre, Shanghai Jiao Tong University, Shanghai 200240, China

**Corresponding author: pengyuan@sjtu.edu.cn*

Received October 8, 2016; accepted December 15, 2016; posted online January 16, 2017

Back conversion is an intrinsic phenomenon in nonlinear frequency down-conversion processes. However, the physical reason for its occurrence is not well understood. Here, we theoretically reveal that back conversion is the result of a π-phase jump associated with the depletion of one interacting wave. By suppressing the idler phase jump through a deliberate crystal absorption, the back conversion can be inhabited, thus enhancing the conversion efficiency from the pump to the signal. The results presented in this Letter will further the understanding of nonlinear parametric processes and pave the way toward the design of highly efficient down-conversion systems.

OCIS codes: 190.4223, 190.4975, 190.7110.
doi: 10.3788/COL201715.021901.

Optical quadratic nonlinear processes, such as sum-frequency generation (SFG), difference-frequency generation (DFG), and optical parametric amplification (OPA), provide a powerful and flexible tool for generating coherent light in the spectral regions inaccessible to laser emissions. One important merit of such quadratic three-wave nonlinear interactions lies in their outstanding designability. On the one hand, various phase-matching schemes can be applied, including quasi-phase matching (QPM)[1–3], adiabatic phase matching[4], and multistep cascade phase matching[5,6]. On the other hand, nonlinear crystals can also be fabricated with distinct structures, including periodically poled grating patterns[1–3] and sectional tiling[2,7], and can be doped with rare-earth ions[8,9].

One inherent characteristic of quadratic nonlinear processes is that they allow both forward and backward energy transfers among the interacting waves in the crystal[10]. Such back conversion will be detrimental when a unidirectional energy transfer is desired. It is well known that phase mismatch among the interacting waves can cause back conversion, which can be prevented using QPM[1–3]. Under the perfect phase-matching conditions, however, back conversion can still occur when one interacting wave is depleted. This back conversion will set an ultimate limit on the application performance of a quadratic nonlinear process[11–14]. As of now, the physical reason for the occurrence of this back conversion is still unclear, and there is still no effective method to inhibit it.

One can usually answer the most basic and important questions about optics through the phase of a wave. A phase jump of π widely exists in linear optics, such as the half-wave loss associated with an interface reflection and the Gouy phase-shift associated with beam focusing[15,16]. In this Letter, we numerically find an analog of this phase jump in nonlinear optics, which occurs when one wave is completely depleted in the process of three-wave interactions. This nonlinear phase jump is indeed the origin of back conversion in a phase-matched DFG process. From this new perspective, we can explore a method to inhibit such a back conversion, which has long been regarded as impossible. For a parametric down-conversion process, such as DFG or OPA, the back conversion can be inhibited by removing the phase jump of the idler wave through deliberate crystal absorption. Our studies would be beneficial for a deep understanding of optical quadratic nonlinear processes and pave the way toward the design of highly efficient DFG systems.

We start with the standard nonlinear coupled-wave equations that govern three-wave interactions (represented by W_1, W_2, and W_3, with the angular frequencies $\omega_1 < \omega_2 < \omega_3, \omega_1 + \omega_2 = \omega_3$)[10],

$$\frac{dA_1}{dz} = -i\frac{\omega_1 d_{\text{eff}}}{n_1 c} A_2^* A_3 e^{-i\Delta kz}, \tag{1}$$

$$\frac{dA_2}{dz} = -i\frac{\omega_2 d_{\text{eff}}}{n_2 c} A_1^* A_3 e^{-i\Delta kz}, \tag{2}$$

$$\frac{dA_3}{dz} = -i\frac{\omega_3 d_{\text{eff}}}{n_3 c} A_1 A_2 e^{i\Delta kz}, \tag{3}$$

where $A_j(z) = \rho_j(z)\exp[i\varphi_j(z)]$ is the electric field envelope, and ρ_j and φ_j refer to the amplitude and phase, respectively. n_j is the refractive index of the crystal, d_{eff} is the effective nonlinear coefficient, and c is the light speed in a vacuum. $\Delta k = k_3 - k_2 - k_1$ is the wave-vector mismatch among the three interacting waves. After defining a total phase $\theta = \Delta kz - \varphi_3(z) + \varphi_2(z) + \varphi_1(z)$, employing the transformation $e^{i\theta} = \cos\theta + i\sin\theta$, and equating the real and imaginary parts, Eqs. (1)–(3) become

$$\frac{d\rho_1}{dz} = -\frac{\omega_1 d_{\text{eff}}}{n_1 c}\rho_2\rho_3 \sin\theta, \tag{4}$$

$$\frac{d\rho_2}{dz} = -\frac{\omega_2 d_{\text{eff}}}{n_2 c}\rho_1\rho_3 \sin\theta, \tag{5}$$

$$\frac{d\rho_3}{dz} = \frac{\omega_3 d_{\text{eff}}}{n_3 c}\rho_1\rho_2 \sin\theta, \tag{6}$$

$$\frac{d\varphi_1}{dz} = -\frac{\omega_1 d_{\text{eff}}}{n_1 c}\frac{\rho_2\rho_3}{\rho_1} \cos\theta, \tag{7}$$

$$\frac{d\varphi_2}{dz} = -\frac{\omega_2 d_{\text{eff}}}{n_2 c}\frac{\rho_1\rho_3}{\rho_2} \cos\theta, \tag{8}$$

$$\frac{d\varphi_3}{dz} = -\frac{\omega_3 d_{\text{eff}}}{n_3 c}\frac{\rho_1\rho_2}{\rho_3} \cos\theta. \tag{9}$$

From Eqs. (4)–(6), we can see that the direction of the energy flow among the three interacting waves is determined by $\sin\theta$. When $\sin\theta < 0 (d\rho_3/dz < 0, d\rho_1/dz > 0, d\rho_2/dz > 0)$, the energy flow is from wave W_3 to waves W_1 and W_2 (i.e., $W_3 \rightarrow W_1 + W_2$). When $\sin\theta > 0 (d\rho_3/dz > 0, d\rho_1/dz < 0, d\rho_2/dz < 0)$, the energy flow is inverse, i.e., $W_1 + W_2 \rightarrow W_3$. From the definition of θ, a phase accumulation due to Δk can induce the symbol change of $\sin\theta$, so a phase mismatch can cause the back conversion. However, here we only consider the perfect phase-matching condition ($\Delta k = 0$). In this case, $\sin\theta = \sin[\varphi_1(z) + \varphi_2(z) - \varphi_3(z)]$, that is, the direction of the energy flow depends on the phase changes of the three interacting waves. Let us consider a DFG process, in which only W_2 and W_3 are seeded onto the crystal. The initial phases of these two waves are assumed to be equal to zero, i.e., $\varphi_2(0) = 0$, and $\varphi_3(0) = 0$. In this case, the newly generated wave W_1 accommodates its phase to $\varphi_1(0) = -\pi/2$ in order to maximize the conversion rate from W_3 to W_1 and $W_2 (\sin\theta = -1)$. As there is no phase mismatch, $\sin\theta$ remains at a value of -1 until the pump W_3 is completely depleted at a position $z = L_0$. From Eq. (9), when $\rho_3 = 0$, $d\varphi_3/dz \rightarrow \infty$, so there exists a phase jump on φ_3. This phase jump activates the back conversion in the SFG. From Eqs. (4)–(6), to maximize the rate of such a back conversion, it requires $\sin\theta = 1$, i.e., $\varphi_1(L_0) + \varphi_2(L_0) - \varphi_3(L_0) = \pi/2$. As $\varphi_1(L_0) = -\pi/2$ and $\varphi_2(L_0) = 0$, φ_3 has to jump from 0 to $-\pi$, i.e., $\varphi_3(L_0) = -\pi$. Such a phase jump is the underlying reason for the back conversion. At the position $z = 2L_0$, the idler will be completely depleted. Similar to the above analysis, $\varphi_1(2L_0)$ will jump from $-\pi/2$ to $\pi/2$ to change $\sin\theta$ from 1 to -1 to activate the forward DFG process again. In such a way, the forward and backward conversions happen periodically. Note that the phase of W_2 does not change with the distance during the whole process, because it cannot be depleted at any time.

To verify the above theoretical analysis, we numerically solved Eqs. (1)–(3) by the symmetrized split-step Fourier method. A DFG process with $\lambda_3 = 532$ and $\lambda_2 = 800$ nm in a collinear phase-matched β-BBO crystal orientated at 22.05° was simulated. Pump wave W_3 is a Gaussian pulse with a full width at half-maximum (FWHM) duration of 100 ps, and its peak intensity is 5 GW/cm^2, while the incident signal wave W_2 is a super-Gaussian pulse with an FWHM duration of 240 ps and a peak intensity of 1 GW/cm^2 (Fig. 1). Dispersions, walk-off, and diffraction effects are all neglected in our calculations.

Figure 2 summarizes the calculated intensity and phase evolutions of the three interacting waves in a 10-mm-long

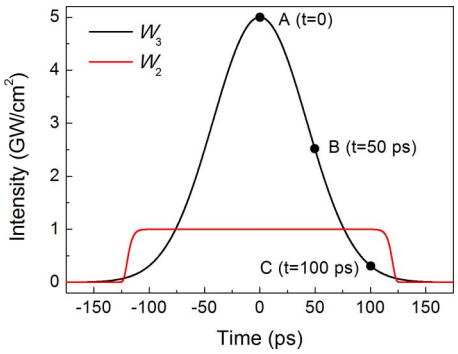

Fig. 1. Pulse profiles of input waves W_3 and W_2. A, B, and C are the three calculation points in the following simulation corresponding to $t = 0$, 50, and 100 ps, respectively.

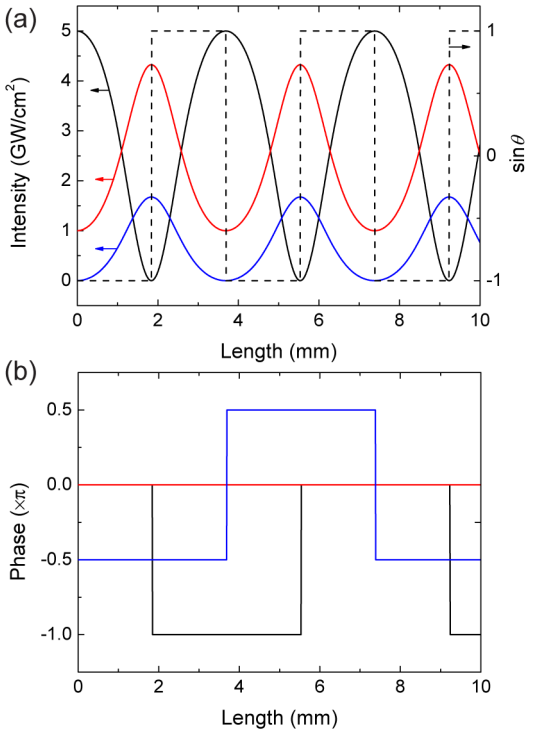

Fig. 2. Intensity and phase evolutions of the three interacting waves. (a) Intensity evolutions of W_1 (blue solid curve), W_2 (red solid curve), and W_3 (black solid curve) within the crystal. The black dashed curve represents the calculated value of $\sin\theta$. (b) Phase evolutions of W_1 (blue curve), W_2 (red curve), and W_3 (black curve) within the crystal. All the intensities and phases in this figure are calculated at point A, as shown in Fig. 1.

β-BBO crystal. Note that these results are calculated at the local temporal coordinate of $t = 0$ (i.e., point A in Fig. 1). As is clearly shown in Fig. 2(a), the direction of the energy flow depends on $\sin\theta$: when $\sin\theta = -1$, $W_3 \rightarrow W_1 + W_2$, and when $\sin\theta = 1$, $W_1 + W_2 \rightarrow W_3$. The sign of $\sin\theta$ changes when one wave is depleted. For example, when W_3 is depleted ($\rho_3 = 0$) at $z = 1.84$ mm, $\sin\theta$ changes from -1 to 1; when W_1 is depleted ($\rho_1 = 0$) at $z = 3.68$ mm, $\sin\theta$ changes from 1 to -1. Through these phase evolutions [Fig. 2(b)], we can see that the full depletion of one wave indeed causes a π-phase jump, which matches our theoretical analysis very well. The phase of W_2 keeps a constant value of zero because it cannot be depleted at any time. This is the reason why the signal phase can be preserved in the DFG.

Although the back conversion process is activated by the phase jump, its occurrence time depends on the coupling intensity of the nonlinear interactions, as implied by Eqs. (4)–(9). In our simulation, because pump pulse W_3 has a Gaussian temporal profile (Fig. 1), back conversion will not take place simultaneously in the temporal domain. Figure 3 shows the intensity evolutions of W_2 at $t = 0$, 50, and 100 ps, respectively. Obviously, the higher pump intensity (e.g., point A) drives an earlier and stronger back conversion. Because the back conversion happens nonuniformly in the temporal domain, the energy of pump wave W_3 (i.e., the integration of all the temporal coordinates) can never be depleted completely, thus significantly degrading the conversion efficiency from W_3 to W_2. The effect of back conversion on the conversion efficiency is more serious in the OPA, which is typically pumped by a spatiotemporally Gaussian laser. To mitigate the back conversion effects, the pump pulses can be shaped to a flat-top profile, or the pump and signal pules can be shaped to the conformal profiles[17,18]. However, these shaping methods are all complicated and are also not applicable to the short-pulse-pumped OPAs.

In most DFG and OPA processes, only one wave (e.g., W_2, the signal) is desirable, with the other wave (e.g., W_1, the idler) as a byproduct. The fundamental method to inhibit the back conversion is to control the phase of W_1. From the above analysis, if the phase of W_1 does not change with the distance, i.e., $\varphi_1(z) = -\pi/2$, the back conversion will no longer happen. This requires that the intensity of W_1 should remain unusually smaller than that predicted by the Manley–Rowe relation[9]. Therefore, the idler wave W_1 must be consumed by an additional process. Linear crystal absorption is one convenient way to deplete W_1. We assume that the absorption coefficient of W_1 is α and rewrite Eq. (1) as

$$\frac{dA_1}{dz} = -i\frac{\omega_1 d_{\text{eff}}}{n_1 c} A_2^* A_3 e^{-i\Delta kz} - \frac{1}{2}\alpha A_1. \tag{10}$$

By numerically solving Eqs. (1)–(3) and (10), the intensity and phase evolutions of the three waves under two absorption levels of $\alpha L_{\text{nl}} = 2$ and 8 are summarized in Fig. 4, where the nonlinear length L_{nl}, as defined in Ref. [18], is fixed at 1.5 mm. By inducing an absorption of $\alpha L_{\text{nl}} = 8$ on W_1, the back conversion indeed no longer happens as expected, as shown in Fig. 4(b). At each position of the crystal, it can be viewed as a DFG process without the incidence of the idler. Therefore, phase φ_1 keeps at $-\pi/2$ across the entire crystal, while φ_2 and φ_3 remain at a constant value of zero [Fig. 4(d)]. In this case, the conversion from W_3 to W_2 becomes unidirectional without back conversion [Fig. 4(b)]. The inhibition of the back conversion process ensures a complete depletion of W_3 and a maximum amplification of W_2.

In the case of $\alpha L_{\text{nl}} = 2$, although the back conversion can still occur initially, it will diminish gradually, as shown in Fig. 4(a). Compared to the case of no absorption in W_1, the depletion of W_1 is enhanced by the absorption, so its phase jump takes place earlier than usual [Fig. 4(c)]. This earlier phase jump activates the forward conversion process before the end of a complete back conversion. In such a way, W_2 still obtains a net gain in one forward–backward conversion process. As a result, W_2 keeps rising with the decreasing oscillation amplitude [Fig. 4(a)]. Finally, W_2

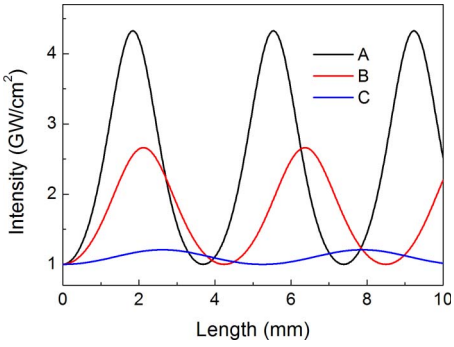

Fig. 3. Intensity evolutions of W_2 at three different temporal points. The black, red, and blue curves correspond to points A, B, and C in Fig. 1, respectively.

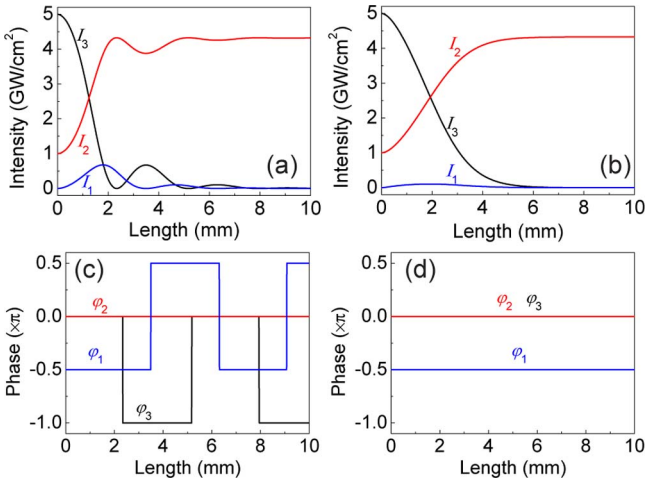

Fig. 4. Intensity and phase evolutions of W_1 (blue curves), W_2 (red curves), and W_3 (black curves) under the conditions of $\alpha L_{\text{nl}} = 2$ [(a) and (c)] and 8 [(b) and (d)]. All calculations correspond to point A in Fig. 1.

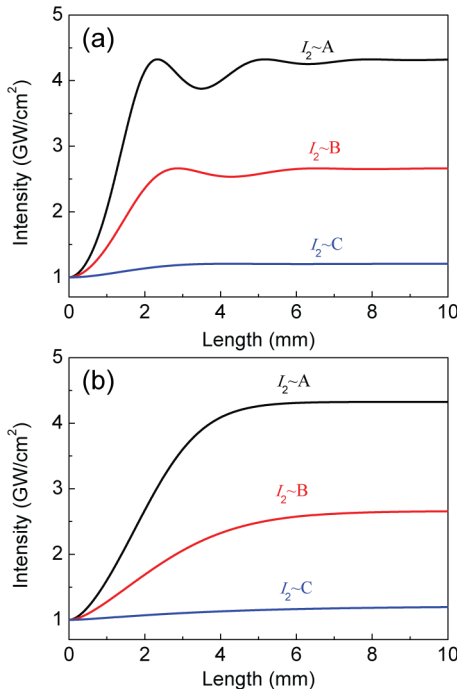

Fig. 5. Intensity evolutions of W_2 under the conditions of $\alpha L_{\mathrm{nl}} =$ (a) 2 and (b) 8. The black, red, and blue curves correspond to points A, B, and C in Fig. 1, respectively.

will approach to the quantum-limited intensity with negligible back conversion, and W_3 is almost completely depleted. In practice, the choice of α depends on the initial pump and signal intensities and also on the crystal length. On the one hand, to effectively suppress the back conversion, the value of α should be larger than a certain value, $\alpha L_{\mathrm{nl}} > m$ ($m = 0.3$ in the case of Ref. [9]). On the other hand, to ensure a maximum conversion efficiency within a limited crystal length L, the value of α should be smaller than a certain value, $\alpha L < n$.

Due to the suppression of the back conversion, each temporal coordinate on W_2 can obtain a maximum gain at the output end of the crystal (Fig. 5), which ensures the maximum conversion efficiency regardless of the profile of W_3. Figure 5 also implies that such a DFG process with absorption in W_1 is robust against the variation of the pump intensity. A more stable output can be expected from such a DFG process without back conversion.

In conclusion, we reveal that the phase jump, accompanied by one depleted interacting wave, is responsible for the intrinsic back conversion in quadratic nonlinear processes. Based on this understanding, we find an effective method to inhabit the back conversion in a parametric down-conversion process. By using crystal absorption to enhance the depletion of the undesirable wave, the back conversion can be terminated, and the conversion efficiency from the pump to the desirable wave could reach the quantum limit. This method for suppressing the back conversion by absorbing the idler wave is compatible with the technique of noncollinear phase matching, so it applies to broadband nonlinear amplification. In the case of broadband amplification, absorption on a specific wavelength (often corresponding to the magic wavelength) can be obtained by doping specific rare-earth ions in an yttrium calcium oxyborate crystal, as we did in Ref. [9]. In addition to the linear absorption method, one could also use a nonlinear method to deplete the undesirable wave, e.g., designing a second-harmonic generation process for this wave in the same crystal[19], which, however, is hard to realize in conventional bulk crystals. The results presented in this study further our understanding of quadratic nonlinear processes and pave the way toward the design of highly efficient parametric down-converters.

This work was supported by the National Basic Research Program of China (No. 2013CBA01505) and the Science and Technology Commission of Shanghai (No. 15XD1502100).

References

1. M. M. Fejer, G. A. Magel, D. H. Jundt, and R. L. Byer, IEEE J. Quantum Electron. **28**, 2631 (1992).
2. J. Ma, Y. Wang, P. Yuan, G. Xie, H. Zhu, and L. Qian, Opt. Lett. **37**, 4486 (2012).
3. P. Hu, G. Li, J. Huo, Y. Zheng, and X. Chen, Chin. Opt. Lett. **13**, 121902 (2015).
4. A. Leshem, G. Meshulam, G. Porat, and A. Arie, Opt. Lett. **41**, 1229 (2016).
5. M. Levenius, M. Conforti, F. Baronio, V. Pasiskevicius, F. Laurell, C. De Angelis, and K. Gallo, Opt. Lett. **37**, 1727 (2012).
6. N. An, H. Ren, Y. Zheng, X. Deng, and X. Chen, Appl. Phys. Lett. **100**, 221103 (2012).
7. B. E. Schmit, N. Thiré, M. Boivin, A. Laramée, F. Poitras, G. Lebrun, T. Ozaki, H. Lbrahim, and F. Légaré, Nat. Commun. **5**, 3643 (2014).
8. S. Longhi, Opt. Lett. **41**, 1813 (2016).
9. J. Ma, J. Wang, P. Yuan, G. Xie, K. Xiong, Y. Tu, X. Tu, E. Shi, Y. Zheng, and L. Qian, Optica **2**, 1006 (2015).
10. R. W. Boyd, *Nonlinear Optics* (Academic press, 2003).
11. I. N. Ross, P. Matousek, G. H. C. New, and K. Osvay, J. Opt. Soc. Am. B **19**, 2945 (2002).
12. J. Moses, C. Manzoni, S.-W. Huang, G. Cerullo, and F. X. Kärtner, Opt. Express **17**, 5540 (2009).
13. J. Ma, J. Wang, D. Hu, P. Yuan, G. Xie, H. Zhu, H. Yu, H. Zhang, J. Wang, and L. Qian, Opt. Express **24**, 23957 (2016).
14. D. Han, Y. Li, J. Du, K. Wang, Y. Li, T. Miyatake, H. Tamiaki, T. Kobayashi, and Y. Leng, Chin. Opt. Lett. **13**, 121401 (2015).
15. E. Hecht, *Optics* (Addison Weley, 2002).
16. S. Feng and H. G. Winful, Opt. Lett. **26**, 485 (2001).
17. L. J. Waxer, V. Bagnoud, I. A. Begishev, M. J. Guardalben, J. Puth, and J. D. Zuegel, Opt. Lett. **28**, 1245 (2003).
18. J. Moses and S.-W. Huang, J. Opt. Soc. Am. B **28**, 812 (2011).
19. G. Porat, O. Gayer, and A. Arie, Opt. Lett. **35**, 1401 (2010).